WESTERN REGION TECHNICAL ATTACHMENT
NO. 99-27
NOVEMBER 23, 1999

THE UTAH WEST DESERT TRAIN TORNADO

Steve Vasiloff - NSSL- NWS WRH/SSD

Introduction

The Salt Lake City WSR-88D (KMTX) can detect trains moving across Utah's west desert in Box Elder County. Technical aspects of this anomalous point target were documented in a Response to *Request for Technical Information (RTI) Number 13343* entitled "Anomalous Target on Salt Lake City WSR-88D" (WSR-88D OSF; 1995). This anomaly is unexpected as one would NOT normally expect a radar located 2300' above the desert terrain to detect trains. However, these train signatures are seen in velocity data and can trigger the WSR-88D Tornado Detection Algorithm creating operational problems for forecasters, especially if storms are present. This Technical Attachment documents a false Tornadic Vortex Signature (TVS) detection on 19 September 1999.

Case Study of a Train-induced TVS

The KMTX WSR-88D is located at Promontory Point, 2300 ft above the surrounding Great Salt Lake (Fig. 1). A Southern Pacific railway passes 2.5 nm to the south of KMTX and extends westward to Nevada (Fig. 2). As shown in RTI No. 13343, the tracks can be seen in the reflectivity, radial velocity, and spectrum width fields (Fig. 3). Note that the WSR-88D has an unobstructed view of the railway to a range of 30 nm and a broken view to a range of about 60 nm. Trains that move along the track are detected by the radar in side lobes. These side lobes are caused by energy bouncing off of various hardware on the radar antenna. While the energy levels in the side lobes are much smaller that in the main lobe, large metal objects, with large back-scattering cross sections, such as trains, planes and trucks, are detectable by side lobes.

Figure 4 shows a typical train signature in both the reflectivity and velocity fields. Near PVC, 40 nm west of KMTX, there is one point of 35 dBZ with surrounding weaker values. All of the radial velocity values are greater than 50 kts. This is the train's velocity signature which can be seen in up to 8 lowest tilts, another characteristic of side lobe contamination. (Fig. 5).

In order for the WSR-88D Tornado Detection Algorithm to issue a TVS detection, a gate-to-gate velocity difference of 11 ms^{-1} must be present on at least 3 tilts and at the lowest tilt. A cell identification is not necessary. A TVS (Fig. 4) was not triggered because there were no in-bound (green) velocities to create a gate-to-gate velocity difference. However, at 2206 UTC on 19 September 1999, radar echoes over the west desert moving toward the radar did provide in-bound velocities to help the train trigger a TVS. Figure 5 shows that a weak cell was present (ID #78). However, a train could not be identified in the reflectivity field. A velocity signature very similar to the one in Fig. 5 was present. Out-bound velocities of greater than 50 kts were adjacent to in-bound velocities which, combined with the vertical structure, caused a TVS alarm.

Discussion

TVS false alarms are, at best, a nuisance. When no storms are present, the forecaster can dismiss them as false and has to only cancel an alarm. However, with storms present, the forecaster must pay close attention to TVS alerts; the alerts must be examined in detail to determine its nature. In the case presented here, the out-bound velocities were unrealistically large with no natural increases to and decreases from the high values, either radially or azimuthally. Even though, upon inspection, these TVS's are obviously false, the alarms are a distraction to operational activities. Furthermore, false alarms in general can reduce forecaster confidence in automated algorithms that are designed to improve operational efficiency.

The nature of TVS false alarms caused by trains suggests that a check could be added to the TDA to filter out spurious velocity values. In the case examined here, there were immediate jumps from near-zero velocities to values over 50 kts. Another strategy would be to increase size thresholds as the train-induced TVS was very small. However, that is not recommended as higher thresholds could cause real TVS signatures to be missed.

Acknowledgments

The author thanks Dale Sirmans of the WSR-88D Operational Support Facility Engineering Branch for technical assistance.

References

WSR-88D Operational Support Facility, 1995: Anomalous target on Salt Lake City WSR-88D. *Response to request for technical information number 13343.* WSR-88D OSF, Norman, OK.

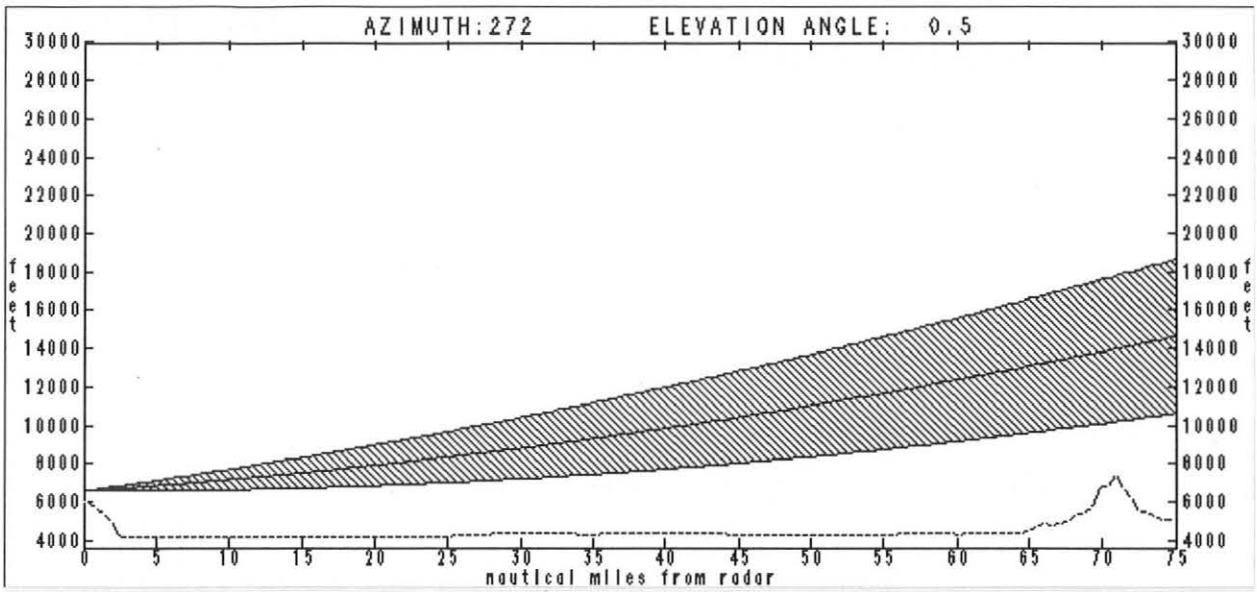

Figure 1. Vertical cross section showing the 0.5 deg beam pattern of the KMTX WSR-88D. The radar is located 2300 ft above the Great Salt Lake. The direction of the cross section is such that the beam is pointing to the west and directly over the Southern Pacific railway.

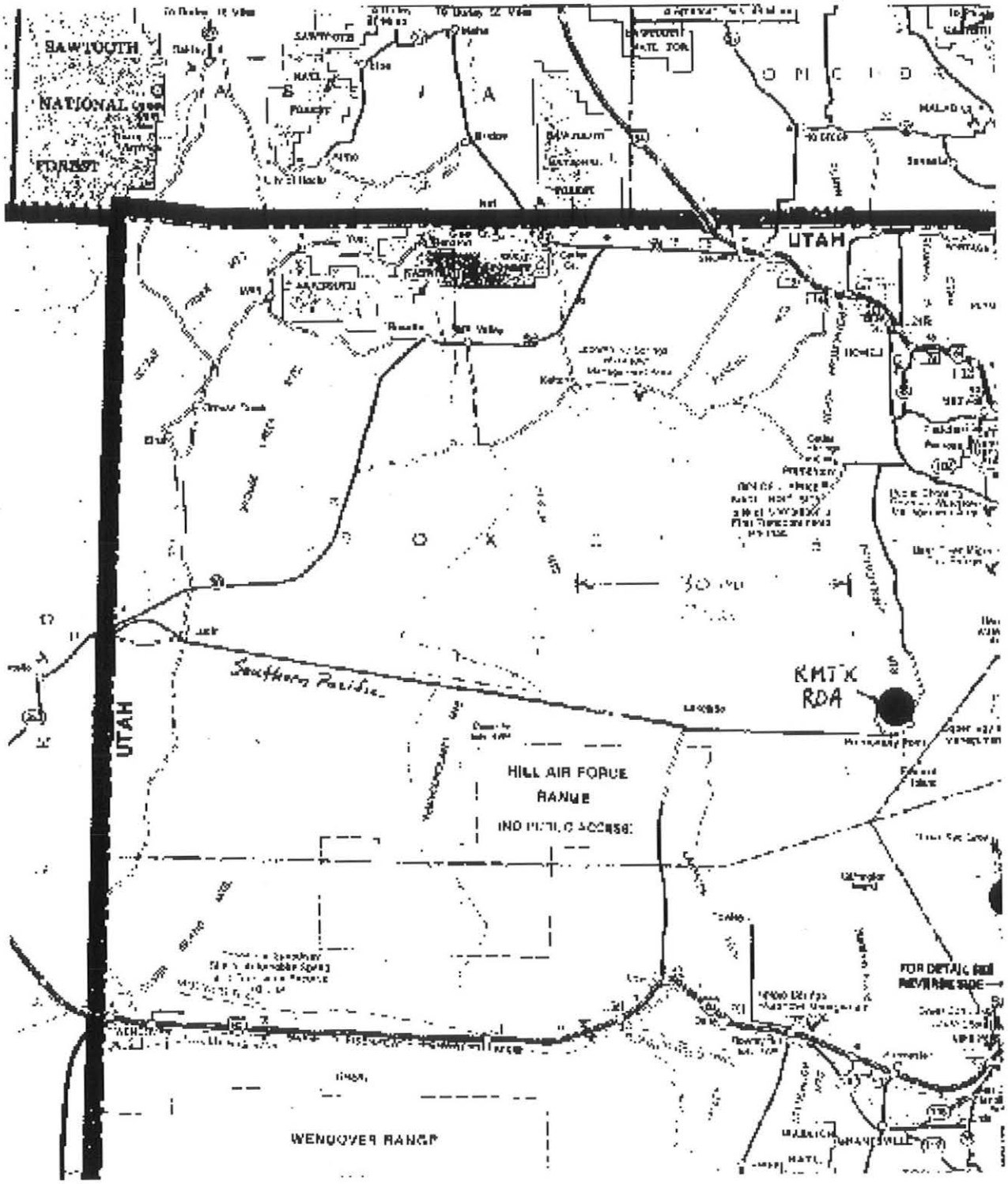

Figure 2. Map of Utah's west desert showing the radar site on Promontory Point and the Southern Pacific railway.

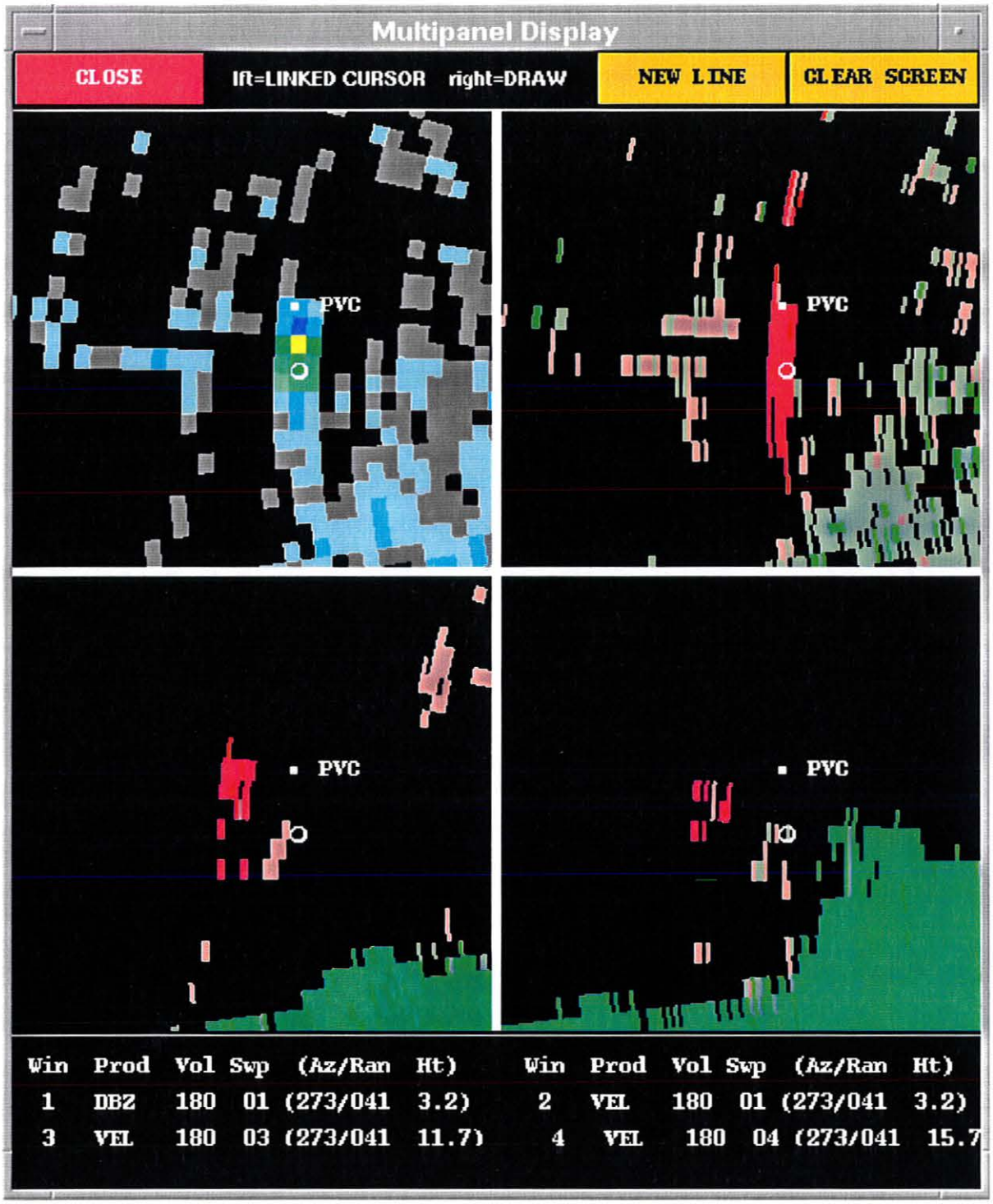

Figure 3. WSR-88D images of a) reflectivity, b) velocity, and c) spectrum width showing the causeway and Southern Pacific tracks across Utah's west desert (from Request for Technical Information (RTI) Number 13343 entitled "Anomalous Target on Salt Lake City WSR-88D" (WSR-88D OSF)). Clutter filters were turned off. The WSR-88D has an unobstructed view of the railway to a range of 30 nm and a broken view to a range of about 60 nm.

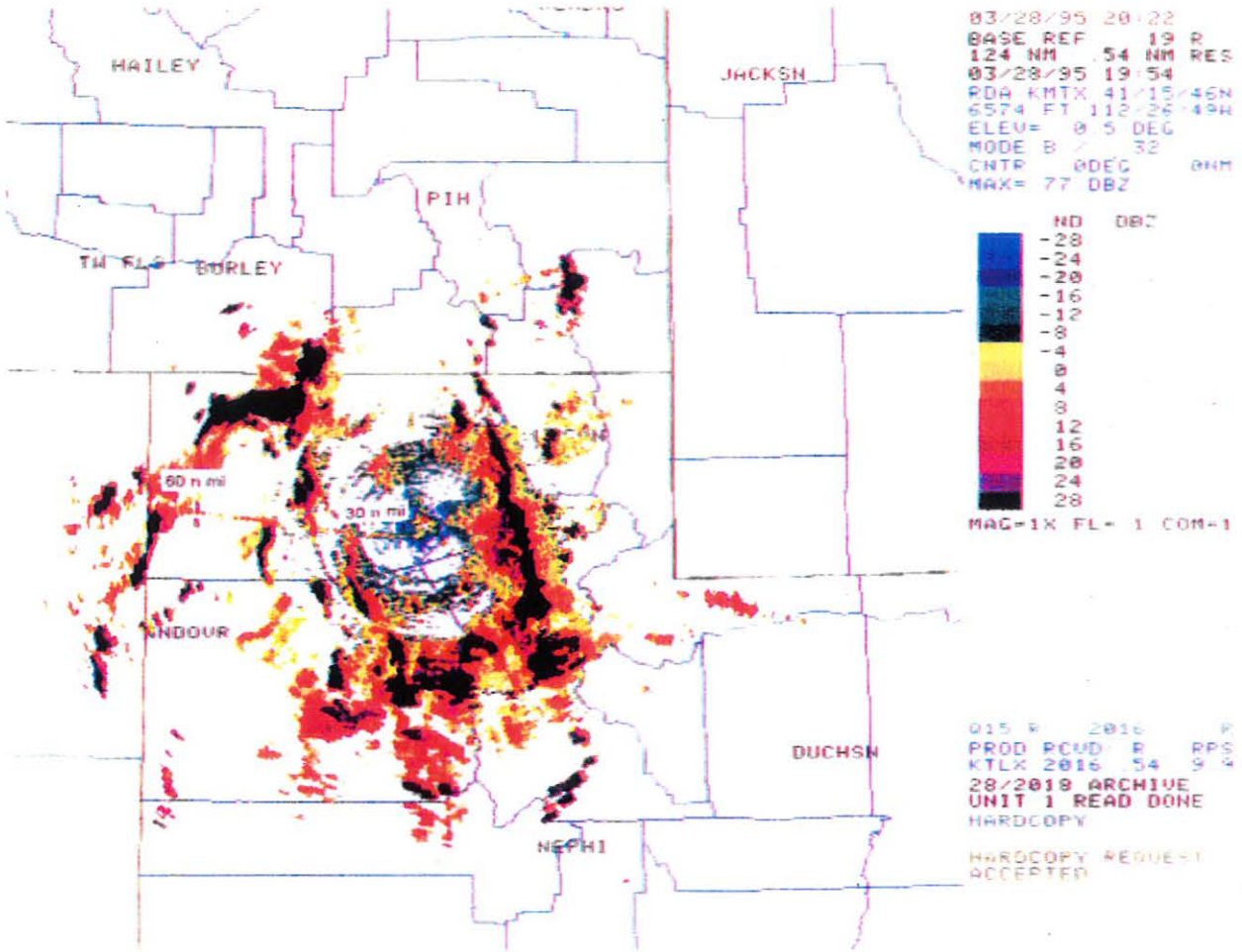

Figure 3a. Radar Display showing causeway and railway. Note that the radar has an unobstructed view of railway to range of about 30 nm and broken view to a range of about 60 nm.

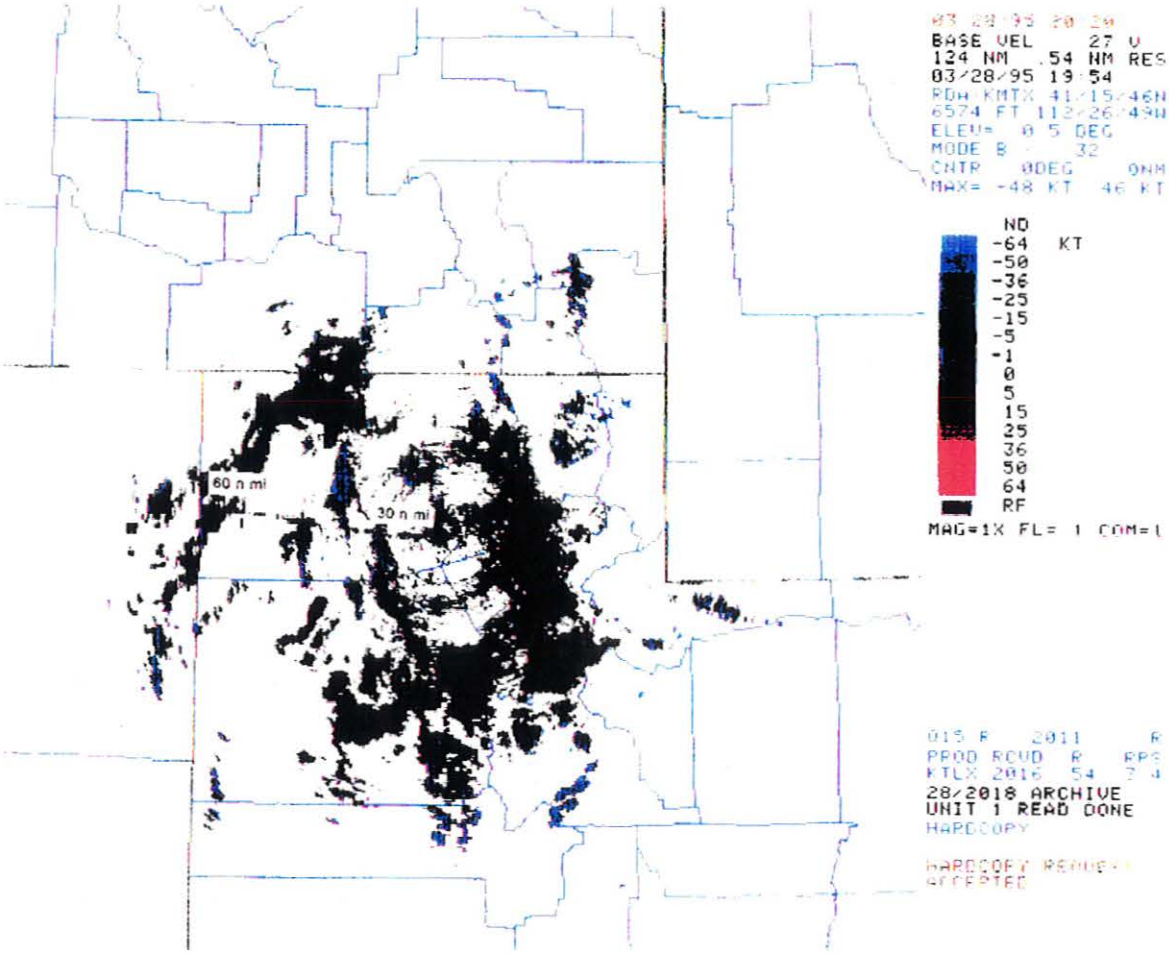

Figure 3b. Radar display showing causeway and railway. Note that the radar has an unobstructed view of railway to range of about 30 nm and broken view to a range of about 60 nm.

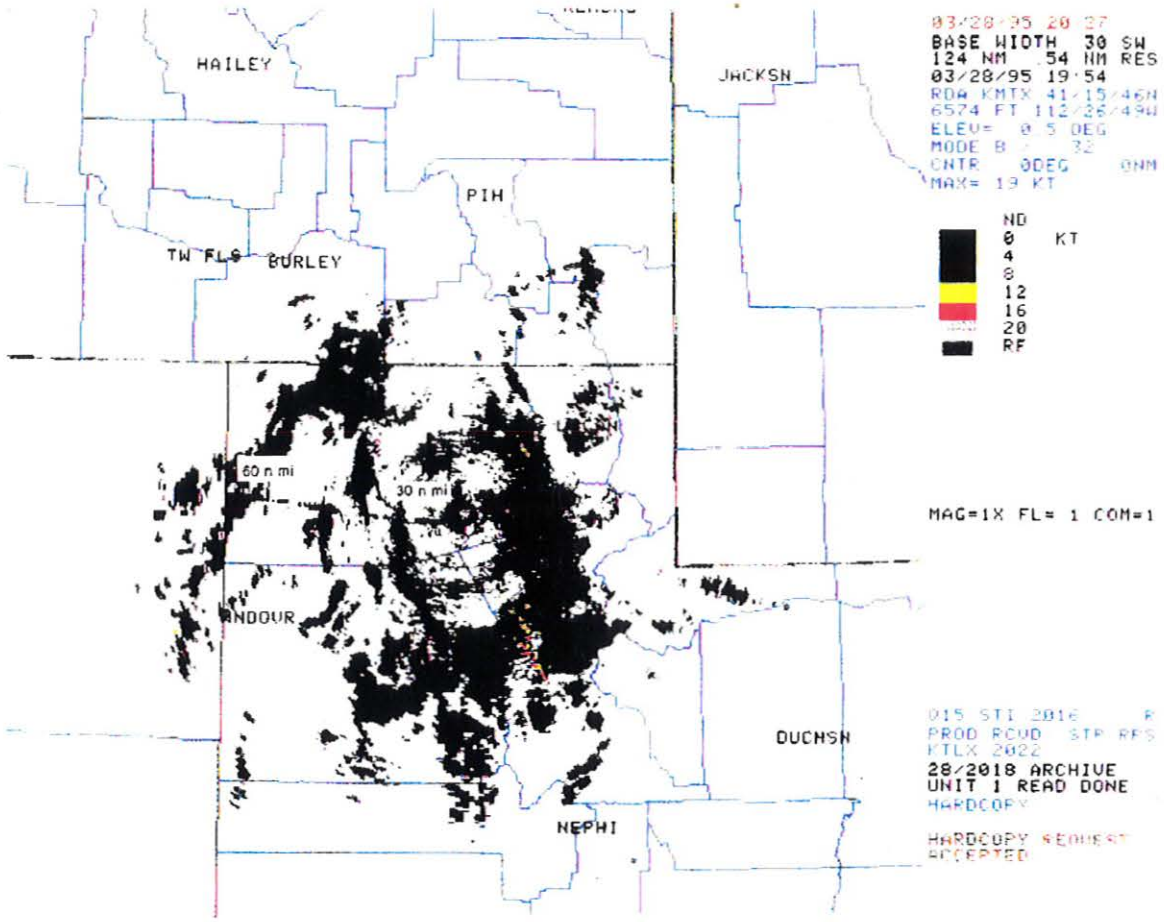

Figure 3c. Radar display showing causeway and railway. Note that the radar has an unobstructed view of railway to range of about 30 nm and broken view to a range of about 60 nm.

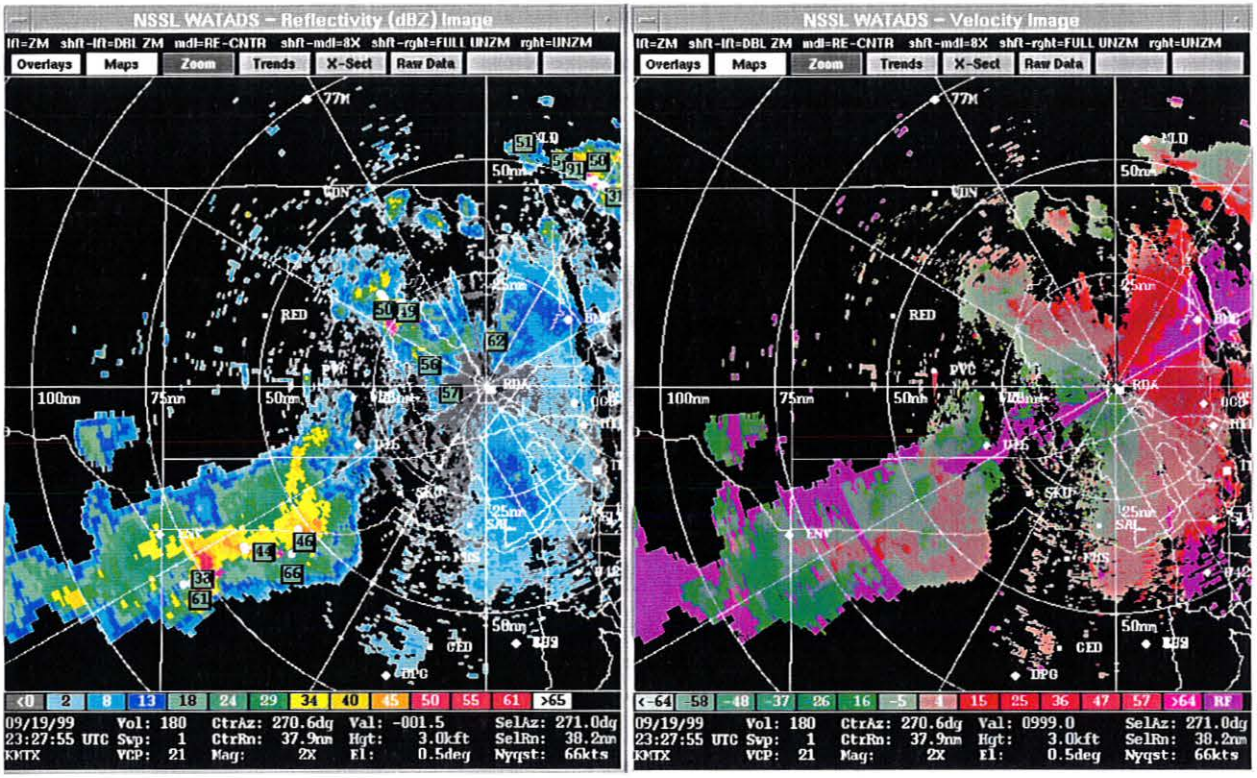

Figure 4. 0.5 deg reflectivity (left) and radial velocity (right) at 2327 UTC showing a typical train echo near PVC due west of the radar.

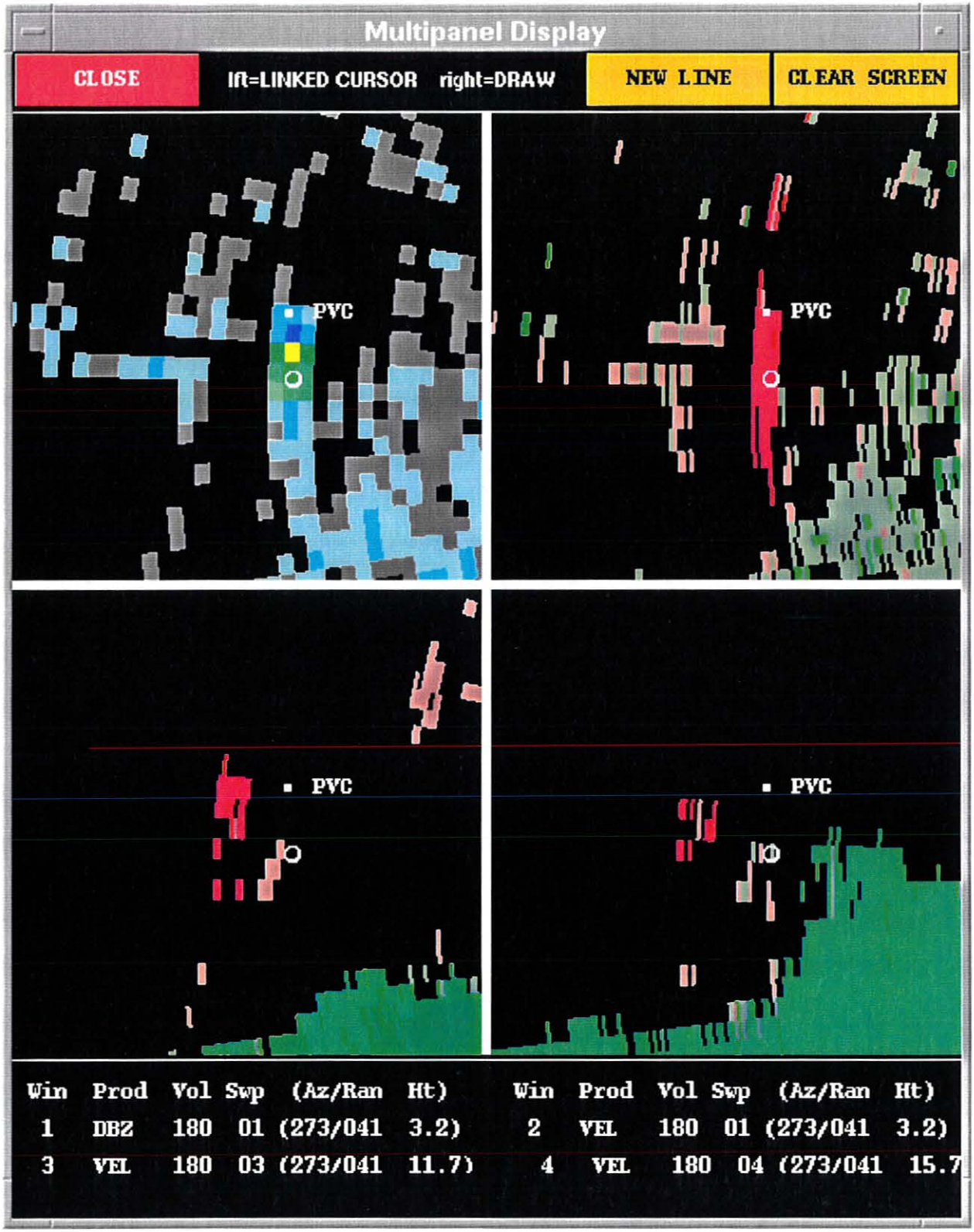

Figure 5. 4-panel of 0.5 deg reflectivity (upper-left), 0.5 deg radial velocity (upper-right), 1.4 deg radial velocity (lower-left), and 2.3 deg radial velocity (lower-right).

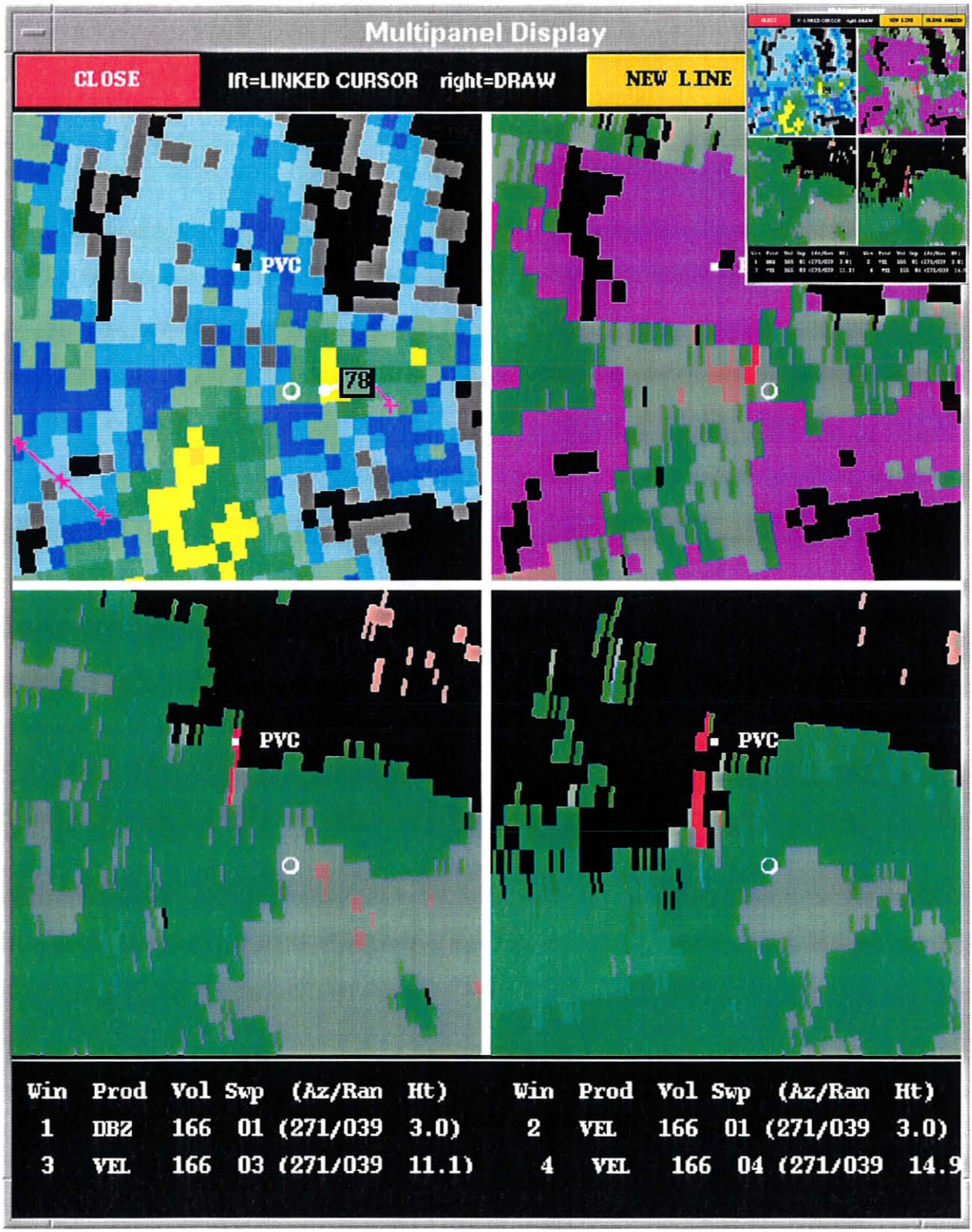

Figure 6. As in Fig. 5, except for 2006 UTC, the time of a TVS detection.

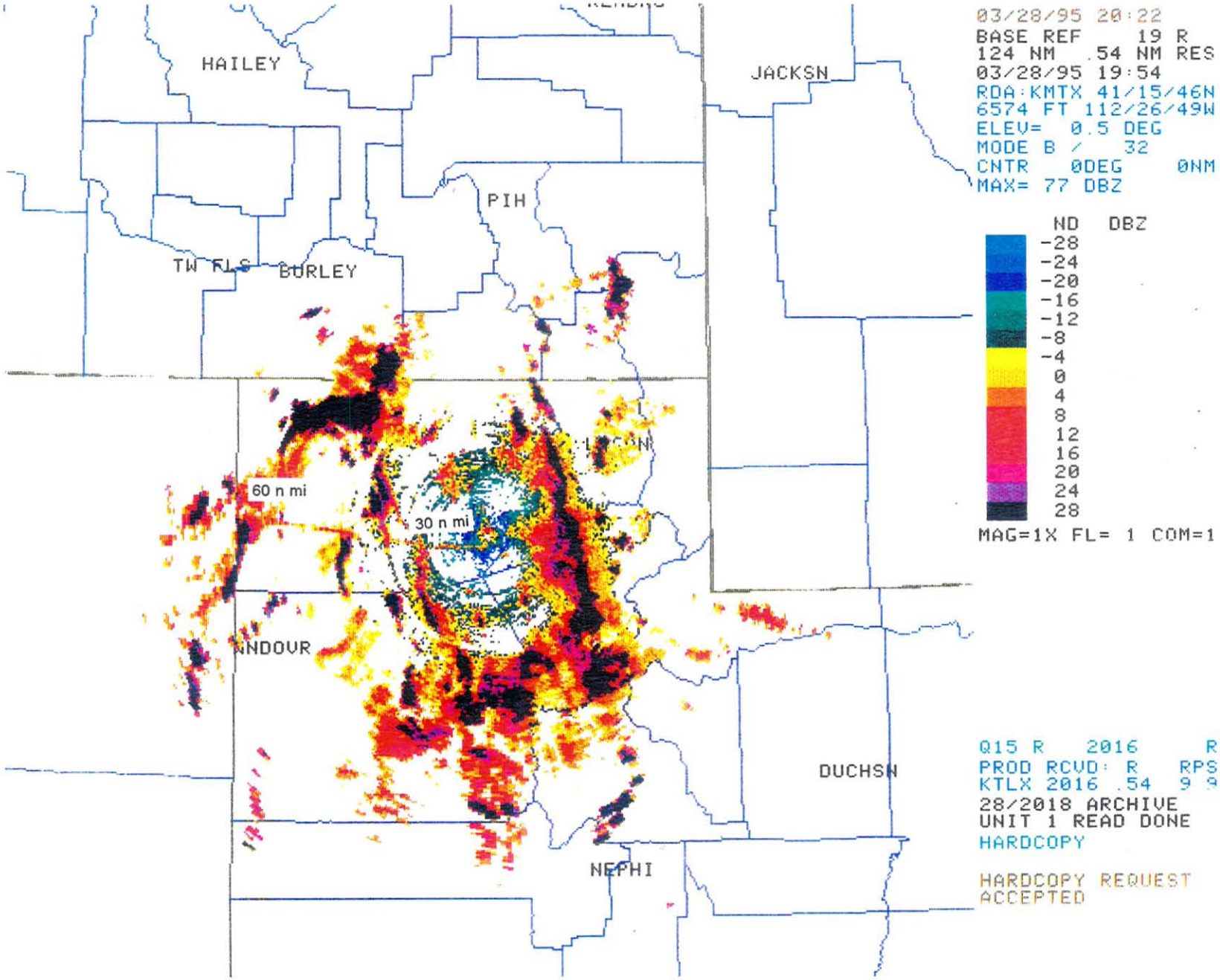

Figure 8.1 Radar display showing causeway and railway. Note that the radar has an unobstructed view of railway to range of about 30 n mi and broken view to a range of about 60 n mi.

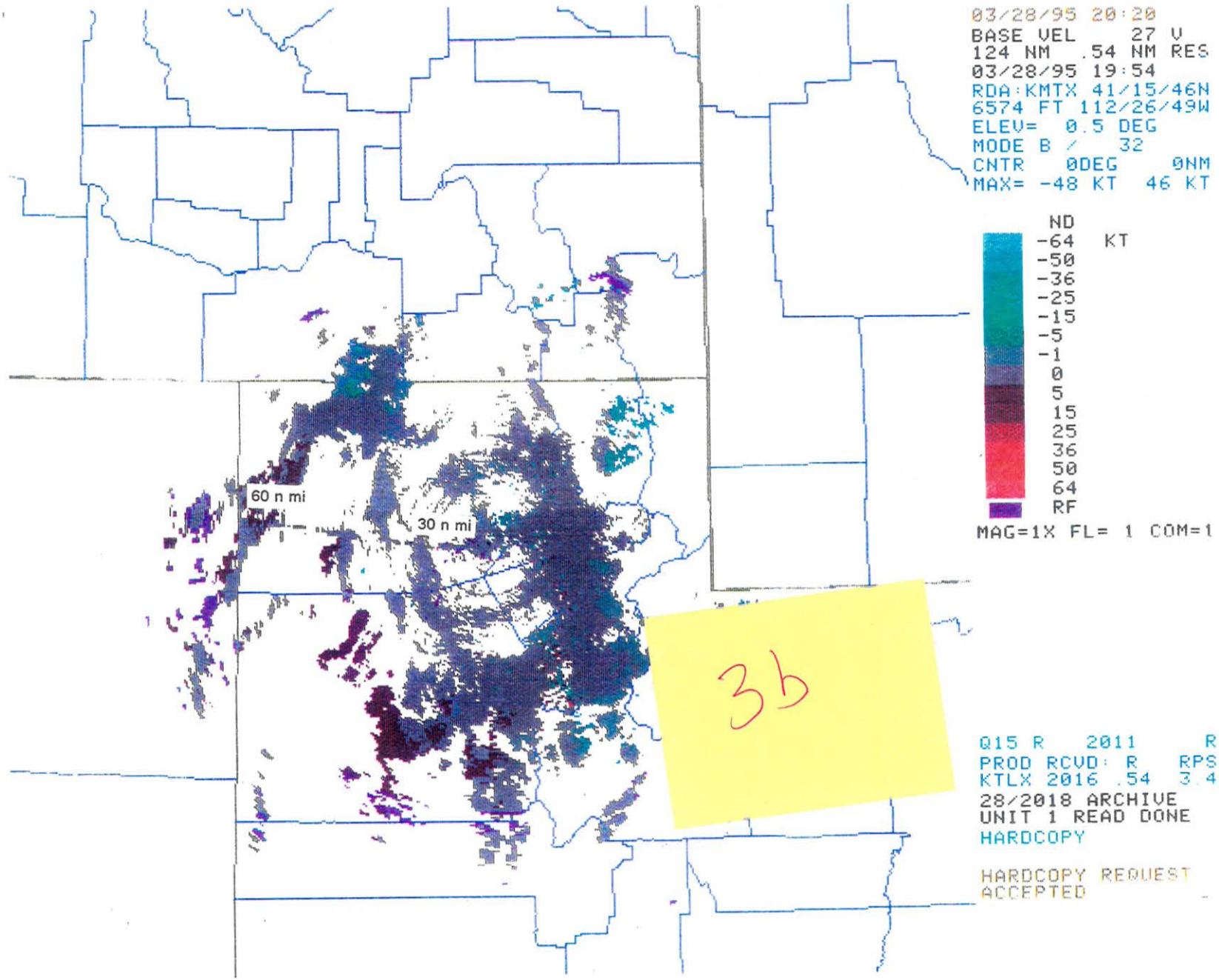

Figure 8.2 Radar display showing causeway and railway. Note that the radar has an unobstructed view of railway to range of about 30 n mi and broken view to a range of about 60 n mi

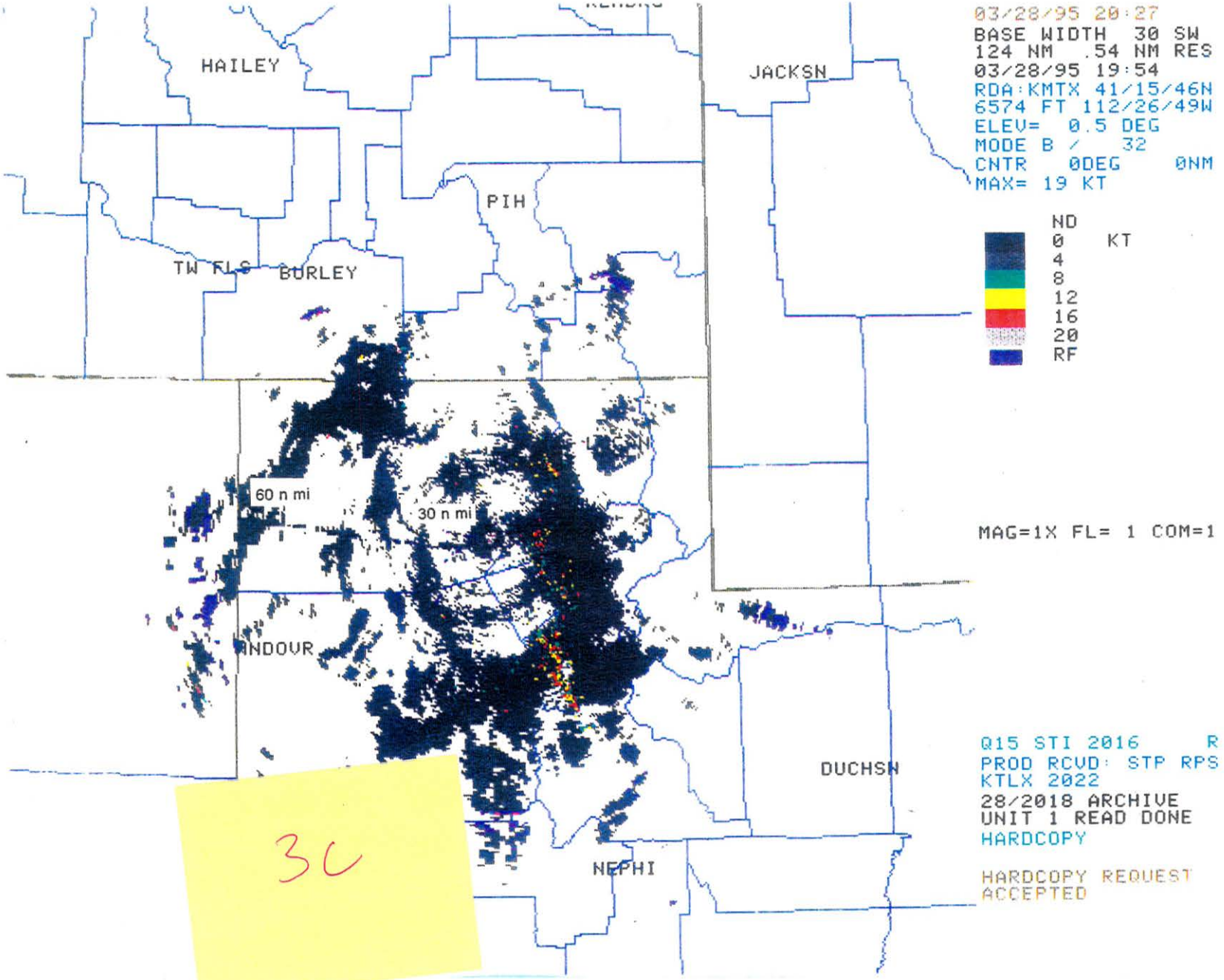

Figure 8.3 Radar display showing causeway and railway. Note that the radar has an unobstructed view of railway to range of about 30 n mi and broken view to a range of about 60 n mi

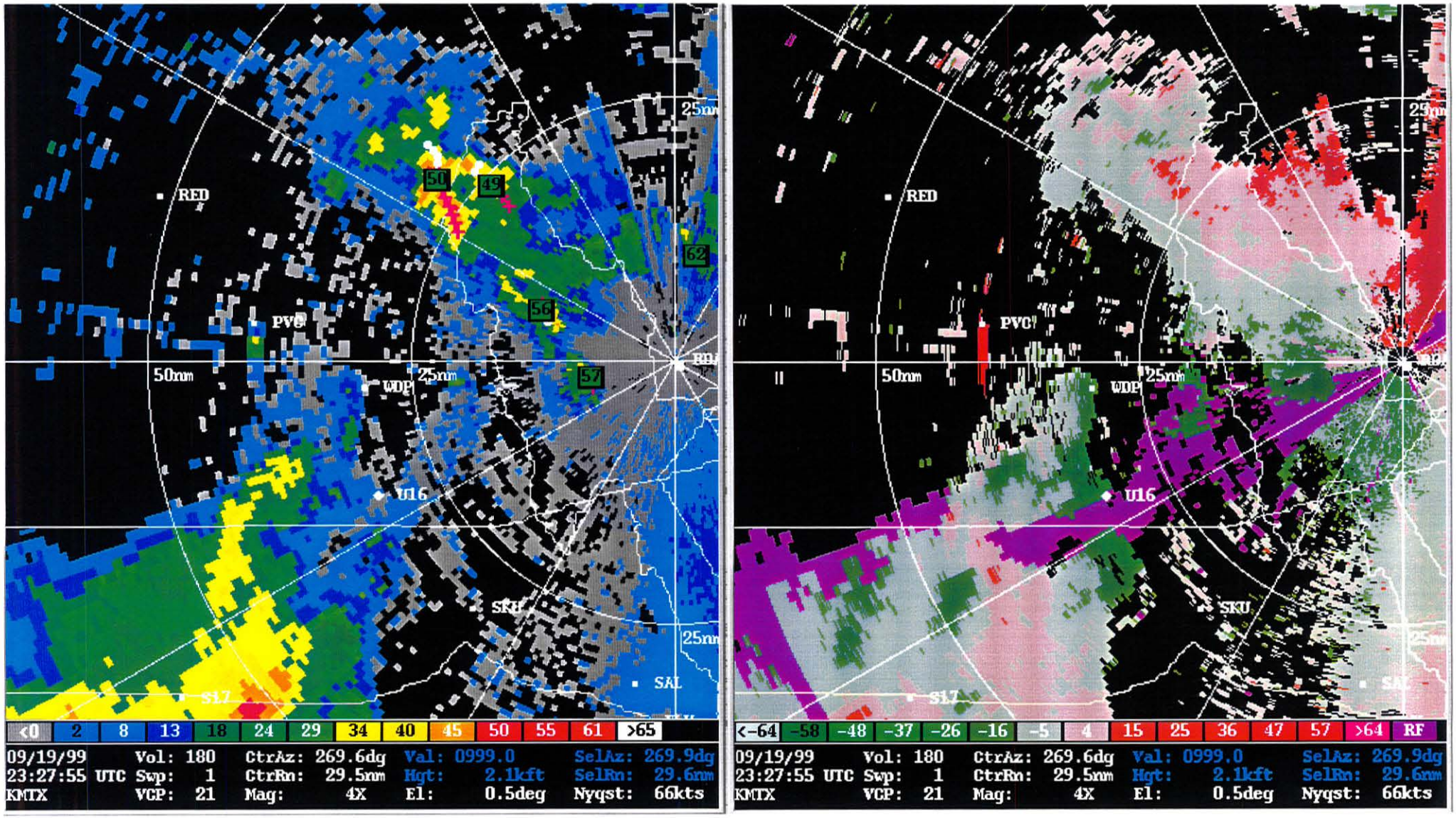
RED
PVC
WDP
U16
SKU
SAL
S17
50nm
25nm
50
49
62
56
57
<0 2 8 13 18 24 29 34 40 45 50 55 61 >65
<-64 -58 -48 -37 -26 -16 -5 4 15 25 36 47 57 >64 RF
09/19/99 Vol: 180 CtrAz: 269.6dg Val: 0999.0 SelAz: 269.9dg
23:27:55 UTC Swp: 1 CtrRn: 29.5nm Hgt: 2.1kft SelRn: 29.6nm
KMTX VCP: 21 Mag: 4X El: 0.5deg Nyqst: 66kts

Figure 4